Nano World Journal

https://doi.org/10.17756/nwj.2022-099

Research Article

Open Access

Poly-Extract Synthesized Silver Nanoparticles Catalysed Rhodamine-B and Methyl Orange Dye Degradation: Influence of Physicochemical Parameters and their Recyclability

Sasikala Vankdoth[1], Aditya Velidandi[2], Mounika Sarvepalli[2] and Meena Vangalapati[1*]

[1]Department of Chemical Engineering, College of Engineering (A), Andhra University, Visakhapatnam, Andhra Pradesh, India

[2]Department of Biotechnology, National Institute of Technology, Warangal, Telangana, India

***Correspondence to:**
Meena Vangalapati
Department of Chemical Engineering
College of Engineering (A), Andhra University
Visakhapatnam, Andhra Pradesh, India
E-mail: meenasekhar2002@yahoo.com

Received: April 13, 2022
Accepted: May 11, 2022
Published: May 13, 2022

Citation: Vankdoth S, Velidandi A, Sarvepalli M, Vangalapati M. 2022. Poly-Extract Synthesized Silver Nanoparticles Catalysed Rhodamine-B and Methyl Orange Dye Degradation: Influence of Physicochemical Parameters and their Recyclability. *J Nanoworld* 8(2): 42-54.

Published by United Scientific Group

Abstract

Poly-extract (equal ratio of tulasi (leaf), neem (leaf) and turmeric (rhizome) aqueous extracts) was used for the synthesis of silver nanoparticles (SNPs). The SNPs were then used for the degradation of rhodamine-B (RhB) and methyl orange (MO) in presence of sodium borohydride (SBH; reducing agent) as nano-catalysts. Influence of four physicochemical parameters such as: nano-catalyst and reducing agent concentration along with temperature and pH of the degradation process were investigated. Maximum degradation was observed at 100 µg (SNPs amount), 20 mg (SBH amount) and at 70 °C for both RhB and MO dyes. Whereas, pH 8 and pH 6 were found to optimum for RhB and MO dyes, respectively. At optimum conditions, SNPs showed 97.41 ± 2.39% degradation with 0.1554 min^{-1} under 24 min and 97.32 ± 2.12% degradation with 0.5017 min^{-1} under 7 min for RhB and MO dyes, respectively. SNPs further showed good recyclability, with 84.22 ± 2.19% (under 7 min) MO dye degradation even after Cycle 6 with 0.2071 min^{-1} as degradation rate. However, SNPs showed low recyclability for RhB dye degradation with only 71.05 ± 2.14% (under 24 min) degradation after Cycle 4 with 0.0556 min^{-1}. It was observed that degradation kinetics was following pseudo-first order kinetics.

Keywords

Dye degradation, Plant extract, Recyclability, Silver nanoparticles

Introduction

Application of hazardous chemicals and synthetic dyes in day to day activities has led to the environmental pollution, which in turn became a global threat [1, 2]. However, manufacturing and application of various hazardous textile dyes has become a significant contributor to the overall economic growth of developing nations [3]. Additionally, application of such hazardous dyes can also cause environmental pollution through the generation of mutagenic or carcinogenic by-products, which are generated during their degradation [4]. Effluents of textile industries contain several types of contaminants such as: heavy metals, organic and inorganic pollutants, which can be released into the surrounding ecosystem [5]. This in turn will affect the health of the living organism. Among the dyes employed for textile use, about 129 dyes were listed by United States Environmental Protection Agency (US-EPA) to cause cancer and are dangerous to all the living organism and ecosystem alike [3]. Globally, the market size of the textile dyes was expected to reach 10.6 billion USD (United States Dollar) by 2025 from 9.24 billion USD in 2020 [6]. Therefore, removal or degradation of these hazardous dyes is essential for the environmental safety and several approaches were already reported by numerous research groups such as: physical, chemical and biological treatments [4, 7-9].

Physical, chemical and biological methods are conventional approaches used for the treatment of textile industrial effluents [3]. Physical treatment methods employ the use of adsorption and radiation methods. Commonly used adsorbents in effluent treatment include: cheap industrial wastes, chitosan, zeolites and activated charcoal. Radiation treatment is carried out by the application of gamma, UV and X-rays. Chemical treatment methods include the application of several reduction and oxidation techniques, which employ different chemicals and organic solvents. Chemical approaches include intricate processes and require expensive chemicals and solvents and also has high energy utilization. Compared to the physicochemical approaches, biological methods employed for the effluent treatment were found to specific for the type of dyes intended to reduce or degrade [10]. In biological methods, novel, economical and eco-friendlier approaches were being developed and applied in order to reduce the adverse side effects and their specificity and efficiency is of great significance [11, 12].

Recently, nanotechnology and nanoscience areas have gained significant research attention due to their practical applicability [13]. Among the various nanomaterials synthesized, studied and reported, metal nanoparticles (NPs) have garnered significant attention due to their superior catalytic properties [14]. NPs have unique properties compared to their bulk counterparts such as: size, shape, high surface area and surface free energy [15-17]. Several metal NPs such as: palladium, platinum, gold, copper, silver, zinc, iron, cobalt, titanium, etc. were synthesized and employed for various applications which include: antimicrobial, anticancer, anti-diabetic, catalytic activity, etc. [14, 15, 18-20]. Among all the metal NPs reported, silver nanoparticles (AgNPs; SNPs) were found to be suitable for their multi-purpose applicability, particularly degradation of textile dyes [21-23]. Compared to other noble metal NPs, SNPs are economical, can be easily synthesized in different shapes and sizes [3, 24]. Parameters involved in the synthesis of SNPs are of great concern which directly affects their performance [3, 4].

As per existing literature, several approaches were reported for the synthesis of SNPs such as: chemical reduction, physical methods, hydrothermal, laser ablation, Sonochemical, electrochemical, sol-gel method and biological methods (plants, microbes, agricultural and domestic waste) [4, 7]. Among the reported approaches, SNPs synthesized from plant extracts (green synthesis) has gained significant research attention due to its eco-friendly nature and single-step synthesis [25, 26]. Hence, this single-step synthesis method has paved the path for various researchers to explore the potential of different plants with diverse phytochemical composition in the synthesis of SNPs and their applicability as nano-catalysts in the degradation of various textile dyes [3, 27-29]. In addition, the approach is found to be economical, simple, easy and environment friendly [25, 26].

Based on the above stated reasons, the present work focuses on the application of poly-extract synthesized SNPs for their catalytic potential in the degradation of textile dyes such as: rhodamine-B (RhB) and methyl orange (MO) in the presence of sodium borohydride (SBH, reducing agent). The objectives of the work were: (i) to determine the role of SNPs in the degradation of RhB and MO dyes, (ii) to investigate the influence of physicochemical parameters such as: nano-catalyst concentration, reducing agent concentration, process pH and process temperature, and lastly (iii) recyclability of the SNPs. The paper also highlights the limitations of the SNPs for their application in real-time scenario as nano-catalysts and clearly states the future research perspectives.

Materials and Methods

The materials and methods section has provided as supplementary information.

Results and Discussion

The degradation of RhB and MO dyes was dependent on several physical and chemical parameters among which, four such parameters were investigated for their role in the degradation of dyes and how they influence the overall degradation process. The parameters studied for their influence on the process were: (i) nano-catalyst (SNPs) concentration, (ii) reducing agent (SBH) concentration, (iii) process temperature and (iv) processpH. The stock solutions of SNPs (2 mg/mL) and dyes (50 mg/ 100 mL) were prepared freshly, before performing the experiment. Details about the influence of physicochemical parameters over the RhB and MO dyes degradation process were presented in table 1 and table 2, respectively.

Nano-catalyst concentration

RhB and MO dyes can't be degraded solely in the presence of a reducing agent such as SBH; therefore they need some support for the transfer of electrons from borohydride ions (BH_4^-) [5, 30]. In addition, for both, dye molecules and BH_4^- ions need a surface to attach and interact with each other, which will be offered by the catalyst. In this regard, the SNPs will play the role of nano-catalysts.

Existing literature has suggested that the concentration of nano-catalyst is directly proportional to the degradation rate of the dyes [5, 31]. The primary reason behind the above statement is that, by increasing the concentration of nano-catalyst there will be an increase in the number of available active sites which exist over the SNPs surface which further increases the transfer of electrons from SBH. This finally leads to the generation hydroxyl and superoxide radicals [5, 31]. Therefore, effect of SNPs concentration on the dye degradation process was determined by performing the RhB and MO dyes degradation at increasing concentrations (25 µg, 50 µg, 75 µg and 100 µg per 5 mL) in the presence of SBH as reducing agent. The experimental conditions were as follows nano-catalyst concentration: 25 µg, 50 µg, 75 µg and 100 µg; reducing agent concentration: 5 mg; process temperature: 37 °C, process pH: 7 and reaction volume: 5 mL.

Based on the results, it was evident that as the concentration of SNPs increased, the time taken for the complete degradation of RhB was reduced (Figure 1g) dye. At 25 µg concentration, the time taken for the total degradation was 86 min, which was later reduced to 75 min (100 µg). However,

Table 1: RhB dye degradation in presence of SNPs and SBH as nano-catalyst and reducing agent, respectively.

SNPs Conc.	SBHConc.	Reaction				Degradation percentage	Rate constant	Correlation coefficient
		Temp.	pH	Time	Vol.			
(µg)	(mg)	(°C)		(min)	(mL)	(%)	(k), min^{-1}	(R^2)
25	5	37	7	75	5	89.43 ± 1.78	0.0318	0.9952
50						92.28 ± 1.19	0.0377	0.9804
75						94.13 ± 2.32	0.0399	0.9582
100						97.78 ± 2.11	0.0526	0.9104
100	5	37	7	55		83.08 ± 2.92	0.0323	0.9827
	10					87.68 ± 1.72	0.0407	0.9802
	15					92.79 ± 2.06	0.0483	0.9395
	20					97.53 ± 2.24	0.0704	0.9006
100	20	40	7	30		67.15 ± 2.18	0.0289	0.9905
		50				72.89 ± 1.77	0.0318	0.9865
		60				78.92 ± 3.19	0.0385	0.9707
		70				97.03 ± 2.05	0.1209	0.9278
100	20	70	2	24		43.45 ± 3.27	0.0227	0.9721
			4			58.50 ± 3.21	0.0369	0.9965
			6			82.04 ± 2.19	0.0756t	0.9614
			8			97.41 ± 2.39	0.1554	0.9019
			10			-	-	-

at 75 min it was observed that about 89.43 ± 1.78%, 92.28 ± 1.19%, 94.13 ± 2.32% and 97.78 ± 2.11% of RhB dye degradation was observed for 25 µg, 50 µg, 75 µg and 100 µg of SNPs (Figure 1c) with the 0.0318 min^{-1}, 0.0377 min^{-1}, 0.0399 min^{-1} and 0.0526 min^{-1} as pseudo-first order rate constants (Figure 1f). As the SNPs concentration increased from 25 µg to 100 µg, the amount of time reduced was 10 min. Time taken for the complete degradation of RhB dye was 86 min, 82 min, 79 min and 75 min for 25 µg (96.55 ± 2.15%), 50 µg (97.03 ± 2.55%), 75 µg (96.89 ± 2.26%) and 100 µg (97.78 ± 2.11%) of SNPs (Figure 1g). Figure 1 presents the details of RhB dye degradation in the presence of SNPs as nano-catalyst at incremental concentrations with SBH as reducing agent.

Based on the results, it was evident that as the concentration of SNPs increased, the time taken for the complete degradation of MO was reduced (Figure 2g) dye. At 25 µg concentration, the time taken for the total degradation was 39 min, which was later reduced to 30 min (100 µg). However, at 30 min it was observed that about 88.64 ± 2.41%, 90.58 ± 1.76%, 91.48 ± 2.50% and 97.56 ± 2.37% of MO dye degradation was observed for 25 µg, 50 µg, 75 µg and 100 µg of SNPs (Figure 2c) with the 0.0769 min^{-1}, 0.0823 min^{-1}, 0.0862 min^{-1} and 0.1273 min^{-1} as pseudo-first order rate constants (Figure 2f). As the SNPs concentration increased from 25 µg to 100 µg, the amount of time reduced was 09 min. Time taken for the complete degradation of MO dye was 39 min, 36 min, 34 min and 30 min for 25 µg (97.07 ± 1.89%), 50 µg (97.44 ± 2.18%), 75 µg (96.33 ± 3.03%) and 100 µg (97.56 ± 2.37%) of SNPs (Figure 2g). Figure 2 presents the details of MO dye degradation in the presence of SNPs as nano-catalyst at incremental concentrations with SBH as reducing agent.

Reducing agent concentration

RhB and MO dyes can't be reduced or degraded only in the presence of SNPs, hence they need a reducing agent such as SBH to make the dye degradation reaction kinetically feasible [5, 30]. The presence of SBH (as reducing agent) along with SNPs (as nano-catalyst) makes the dye degradation reaction possible by providing the necessary electrons required for the formation of free radicals which in turn attack the chromophore structure of the dye molecules [5, 30]. This transfer of electrons is facilitated by the presence of SNPs.

Therefore, effect of SBH concentration on the dye degradation process was determined by performing the RhB and MO dyes degradation at increasing concentrations (5 mg, 10 mg, 15 mg and 20 mg per 5 mL) in the presence of SNPs as nano-catalyst. The experimental conditions were as follows nano-catalyst concentration: 100 µg (defined in section 3.1); reducing agent concentration: 5 mg, 10 mg, 15 mg and 20 mg; process temperature: 37 °C, process pH: 7 and reaction volume: 5 mL.

Table 2: MO dye degradation in presence of SNPs and SBH as nano-catalyst and reducing agent, respectively.

SNPs Conc.	SBHConc.	Reaction				Degradation percentage	Rate constant	Correlation coefficient
		Temp.	pH	Time	Vol.			
(µg)	(mg)	(°C)		(min)	(mL)	(%)	(k), min^{-1}	(R^2)
25	5	37	7	30	5	88.64 ± 2.41	0.0769	0.9483
50						90.58 ± 1.76	0.0823	0.9358
75						91.48 ± 2.50	0.0862	0.9650
100						97.56 ± 2.37	0.1273	0.9036
100	5	37	7	20		77.18 ± 2.83	0.0696	0.9491
	10					81.53 ± 2.69	0.0892	0.9603
	15					86.90 ± 3.14	0.1093	0.9577
	20					96.17 ± 2.61	0.2236	0.9176
100	20	40	7	9		50.54 ± 3.42	0.1248	0.9987
		50				60.81 ± 1.74	0.1411	0.9962
		60				85.63 ± 2.35	0.3211	0.9286
		70				97.19 ± 2.16	0.4736	0.8383
100	20	70	2	7		-	-	-
			4			-	-	-
			6			97.32 ± 2.12	0.5017	0.9108
			8			66.84 ± 2.26	0.1308	0.9751
			10			-	-	-

Based on the results, it was evident that as the concentration of SBH increased, the time taken for the complete degradation of RhB was reduced (Figure 3g) dye. At 5 mg concentration, the time taken for the total degradation was 75 min, which was later reduced to 55 min (20 mg). However, at 55 min it was observed that about 83.08 ± 2.92%, 87.68 ± 1.72%, 92.79 ± 2.06% and 97.53 ± 2.24% of RhB dye degradation was observed for 5 mg, 10 mg, 15 mg and 20 mg of SBH (Figure 3c) with the 0.0323 min^{-1}, 0.0407 min^{-1}, 0.0483 min^{-1} and 0.0704 min^{-1} as pseudo-first order rate constants (Figure 3f). As the SBH concentration increased from 5 mg to 20 mg, the amount of time reduced was 20 min. Time taken for the complete degradation of RhB dye was 75 min, 69 min, 62 min and 55 min for 5 mg (97.93 ± 1.63%), 10 mg (98.47 ± 1.48%), 15 mg (97.69 ± 2.13%) and 20 mg (97.53 ± 2.24%) of SBH (Figure 3g). Figure 3 presents the details of RhB dye degradation in the presence of SBH as reducing agent at incremental concentrations with SNPs as nano-catalyst.

Based on the results, it was evident that as the concentration of SBH increased, the time taken for the complete degradation of MO was reduced (Figure 4g) dye. At 5 mg concentration, the time taken for the total degradation was 30 min, which was later reduced to 20 min (20 mg). However, at 30 min it was observed that about 77.18 ± 2.83%, 81.53 ± 2.69%, 86.90 ± 3.14% and 96.17 ± 2.61% of MO dye degradation was observed for 5 mg, 10 mg, 15 mg and 20 mg of SBH (Figure 4c) with the 0.0696 min^{-1}, 0.0892 min^{-1}, 0.1093 min^{-1} and 0.2236 min^{-1} as pseudo-first order rate constants (Figure 4f). As the SBH concentration increased from 5 mg to 20 mg, the amount of time reduced was 10 min. Time taken for the complete degradation of RhB dye was 30 min, 27 min, 24 min and 20 min for 5 mg (96.51 ± 2.52%), 10 mg (97.21 ± 2.47%), 15 mg (97.25 ± 1.56%) and 20 mg (96.17 ± 2.61%) of SBH (Figure 4g). Figure 4 presents the details of RhB dye degradation in the presence of SBH as reducing agent at incremental concentrations with SNPs as nano-catalyst.

Process temperature

From the existing literature it was evident that, rise in the process temperature will positively affect the dye degradation process [5, 31, 32]. Based on the above statement, dye degradation reaction can be considered as endothermic reaction [31]. The increase in the dye degradation rate in presence of SNPs (as nano-catalyst) and SBH (as reducing agent) can be primarily due to the following reasons: (i) increase in the temperature can cause the molecules to move faster, this in turn can induce the efficient collision between the dye molecules and electrons, (ii) increase in the temperature could increase the porosity of the SNPs, which in turn can increase the number of active sites and total surface area of the nano-catalyst and lastly (iii) it will reduce the viscosity of solution thereby increasing the mobility of dye molecules, BH_4^- ions and SNPs [31].

Based on the above stated reasons, the effect of temperature on the dye degradation process was determined by per-

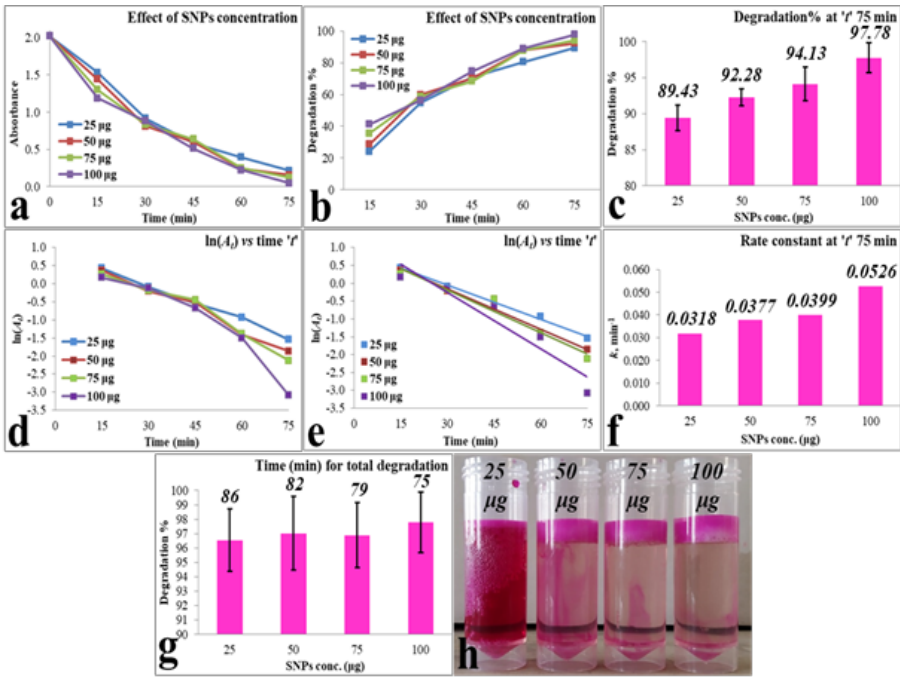

Figure 1: RhB dye degradation at various SNPs concentrations. **(a)** Absorbance values recorded by UV-Vis spec. at 554 nm, **(b)** Degradation% calculated by Eq. 1 (section 2.5.1), **(c)** Degradation% at 75 min, **(d-e)** Ln(A_t) *vs* time '*t*' plot to determine pseudo-first order rate constant, **(f)** Pseudo-first order rate constant values, **(g)** Time taken for total degradation and **(h)** Picture of MO dye degradation at increasing concentrations of SNPs. *Experimental conditions*: SNPs concentration: 25 µg, 50 µg, 75 µg and 100 µg; SBH concentration: 5 mg; Process temperature: 37 °C; Process pH: 7 and Reaction volume: 5 mL (Stock solutions; SNPs: 2 mg/mL and Dye: 50 mg/100 mL).

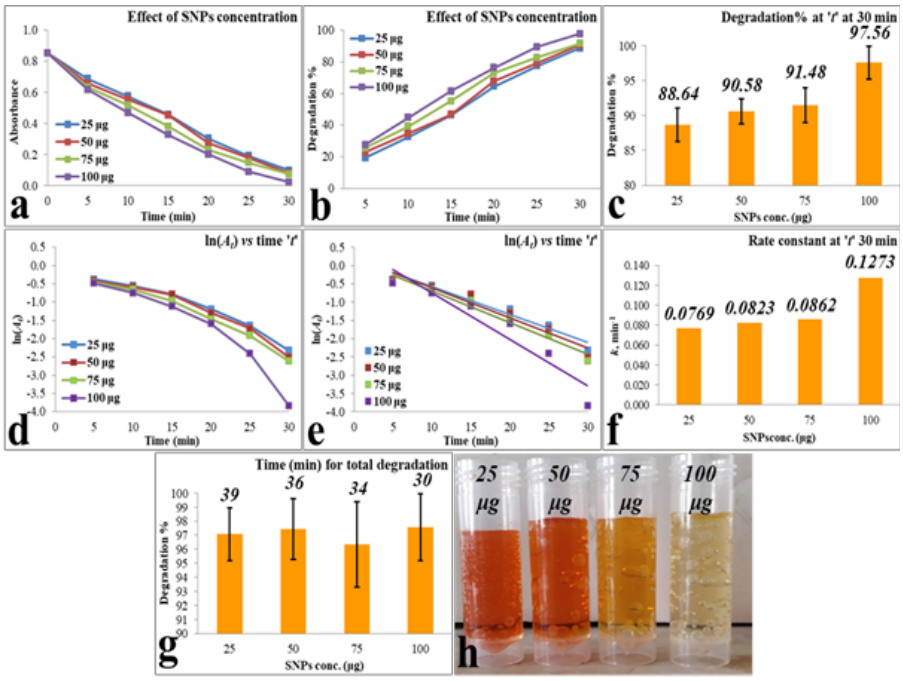

Figure 2: MO dye degradation at various SNPs concentrations. **(a)** Absorbance values recorded by UV-Vis spec. at 464 nm, **(b)** Degradation% calculated by Eq. 1 (section 2.5.1), **(c)** Degradation% at 30 min, **(d-e)** Ln(A_t) *vs* time '*t*' plot to determine pseudo-first order rate constant, **(f)** Pseudo-first order rate constant values, **(g)** Time taken for total degradation and **(h)** Picture of MO dye degradation at increasing concentrations of SNPs. *Experimental conditions*: SNPs concentration: 25 µg, 50 µg, 75 µg and 100 µg; SBH concentration: 5 mg; Process temperature: 37 °C; Process pH: 7 and Reaction volume: 5 mL (Stock solutions; SNPs: 2 mg/mL and Dye: 50 mg/100 mL).

forming the RhB and MO dyes degradation at increasing temperatures (40 °C, 50 °C, 60 °C and 70 °C) in the presence of SNPs and SBH as nano-catalyst and reducing agent, respectively. The experimental conditions were as follows nano-catalyst concentration: 100 µg (defined in section 3.1); reducing agent concentration: 20 mg (defined in section 3.2); process temperature: 40 °C, 50 °C, 60 °C and 70 °C, process pH: 7 and reaction volume: 5 mL.

Based on the results, it was evident that as the process temperature increased, the time taken for the complete degradation of RhB was reduced (Figure 5g) dye. At 40 °C, the time taken for the total degradation was 55 min, which was later reduced to 30 min (at 70 °C). However, at 30 min it was observed that about 67.15 ± 2.18%, 72.89 ± 1.77%, 78.92 ± 3.19% and 97.03 ± 2.05% of RhB dye degradation was observed for 40 °C, 50 °C, 60 °C and 70 °C temperature (Figure 5c) with the 0.0289 min^{-1}, 0.0318 min^{-1}, 0.0385 min^{-1} and 0.1209 min^{-1} as pseudo-first order rate constants (Figure 5f). As the process temperature increased from 40 °C to 70 °C, the amount of time reduced was 25 min. Time taken for the complete degradation of RhB dye was 55 min, 47 min, 37 min and 30 min for 40 °C (98.19 ± 1.76%), 50 °C (97.87 ± 2.03%), 60 °C (97.92 ± 1.94%) and 70 °C (97.03 ± 2.05%) of process temperature (Figure 5g). Figure 5 presents the details of RhB dye degradation at increasing process temperatures in the presence of SBH as reducing agent and SNPs as nano-catalyst.

Based on the results, it was evident that as the process temperature increased, the time taken for the complete degradation of MO was reduced (Figure 6g) dye. At 40 °C, the time taken for the total degradation was 20 min, which was later reduced to 9 min (at 70 °C). However, at 9 min it was observed that about 50.54 ± 3.42%, 60.81 ± 1.74%, 85.63 ± 2.35% and 97.19 ± 2.16% of MO dye degradation was observed for 40 °C, 50 °C, 60 °C and 70 °C temperature (Figure 6c) with the 0.1248 .

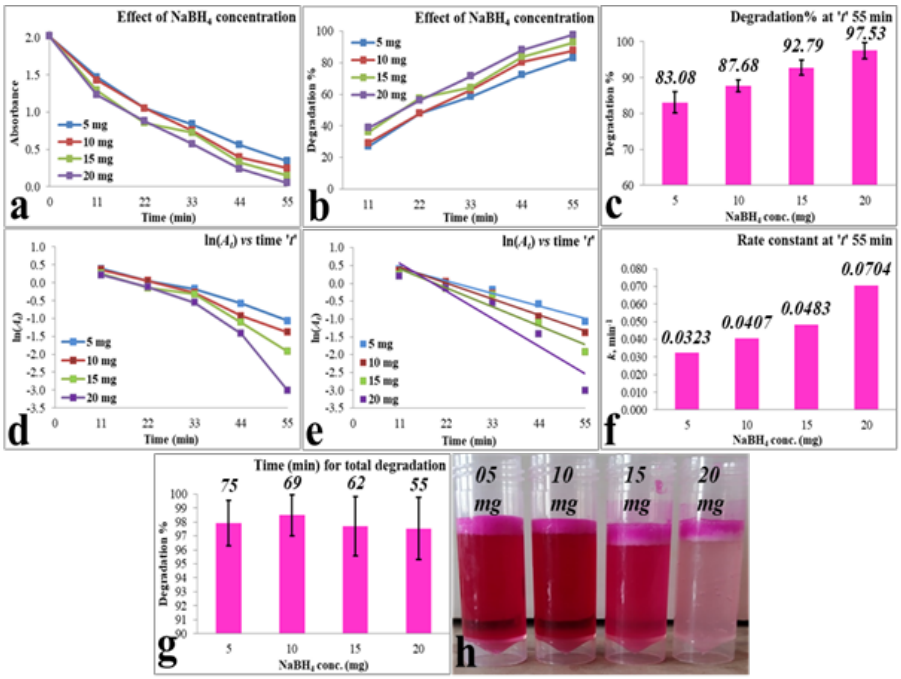

Figure 3: RhB dye degradation at various SBH concentrations. **(a)** Absorbance values recorded by UV-Vis spec. at 554 nm, **(b)** Degradation% calculated by Eq. 1 (section 2.5.1), **(c)** Degradation% at 55 min, **(d-e)** Ln(A_t) *vs* time '*t*' plot to determine pseudo-first order rate constant, **(f)** Pseudo-first order rate constant values, **(g)** Time taken for total degradation and **(h)** Picture of MO dye degradation at increasing concentrations of SBH. *Experimental conditions*: SNPs concentration: 100 µg; SBH concentration: 5 mg, 10 mg, 15 mg and 20 mg; Process temperature: 37 °C; Process pH: 7 and Reaction volume: 5 mL (Stock solutions; SNPs: 2 mg/mL and Dye: 50 mg/100 mL).

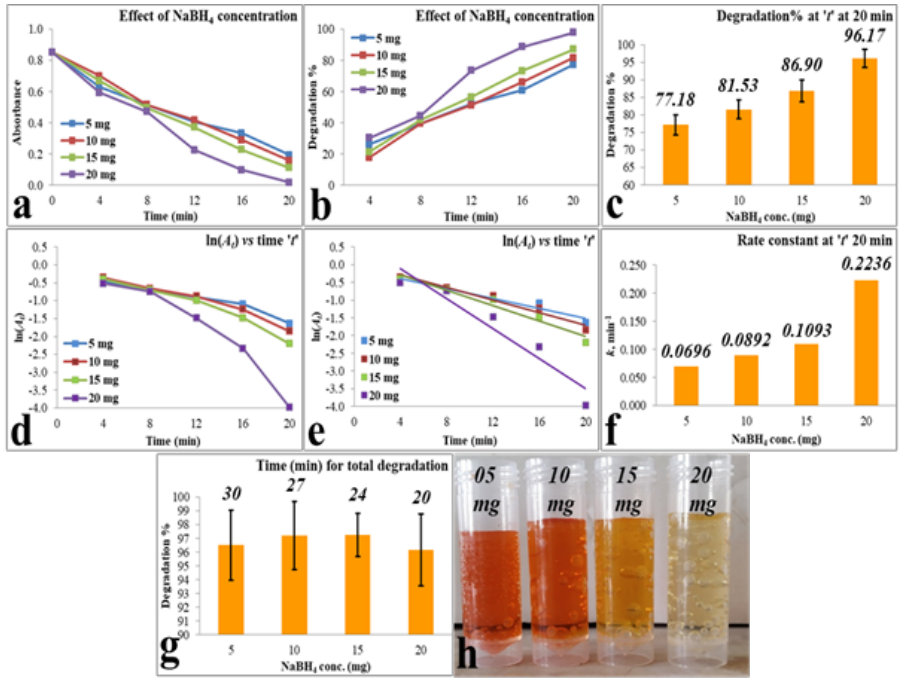

Figure 4: MO dye degradation at various SBH concentrations. **(a)** Absorbance values recorded by UV-Vis spec. at 464 nm, **(b)** Degradation% calculated by Eq. 1 (section 2.5.1), **(c)** Degradation% at 20 min, **(d-e)** Ln(A_t) *vs* time '*t*' plot to determine pseudo-first order rate constant, **(f)** Pseudo-first order rate constant values, **(g)** Time taken for total degradation and **(h)** Picture of MO dye degradation at increasing concentrations of SBH. *Experimental conditions*: SNPs concentration: 100 µg; SBH concentration: 5 mg, 10 mg, 15 mg and 20 mg; Process temperature: 37 °C; Process pH: 7 and Reaction volume: 5 mL (Stock solutions; SNPs: 2 mg/mL and Dye: 50 mg/100 mL).

Process pH

Of all the physicochemical parameters affecting the dye degradation process, pH of the process is considered to be significant [31, 33, 34]. Determining the exact effect of pH over the dye degradation process is considered as a complicated procedure as it will cause multiple effects during the degradation process [31]. As per existing literature, pH can affect the (i) ionization state of the SNPs, (ii) reactive nature of the dye molecules: surface charge of the SNPs in turn resulting in affecting their stability and lastly (iii) nature of the products formed after the dye degradation [31, 35]. Additionally, pH can also affect the production of free radicals by interfering with the electron transfer from BH_4^- ions and SNPs [35].

Based on the above stated reasons, the effect of pH on the dye degradation process was determined by performing the RhB and MO dyes degradation at various pH (2, 4, 6, 8 and 10) in the presence of SNPs and SBH as nano-catalyst and reducing agent, respectively. The experimental conditions were as follows nano-catalyst concentration: 100 µg (defined in section 3.1); reducing agent concentration: 20 mg (defined in section 3.2); process temperature: 70 °C (defined in section 3.3), process pH: 2, 4, 6, 8 and 10 and reaction volume: 5 mL.

At pH 8, maximum dye degradation (97.41 ± 2.39%) was observed in less than 24 min with 0.1554 min^{-1} as degradation rate (Figure 7c and 7f). However, pH 2, pH 4 and pH 6 showed only 43.45 ± 3.27%, 58.50 ± 3.21% and 82.04 ± 2.19% RhB dye degradation with 0.0227 min^{-1}, 0.0369 min^{-1} and 0.0756 min^{-1} as degradation rate, whereas pH 10 showed no dye degradation activity (Figure 7c, 7f and 7h). Total degradation of RhB dye was observed under 53 min, 42 min and 31 min for pH 2 (97.68 ± 1.87%), pH 4 (97.72 ± 2.11%) and pH 6 (98.35 ± 1.66%), respectively (Figure 7g). Figure 7 presents the details of RhB dye degradation at various process pH in the presence of SBH as reducing agent

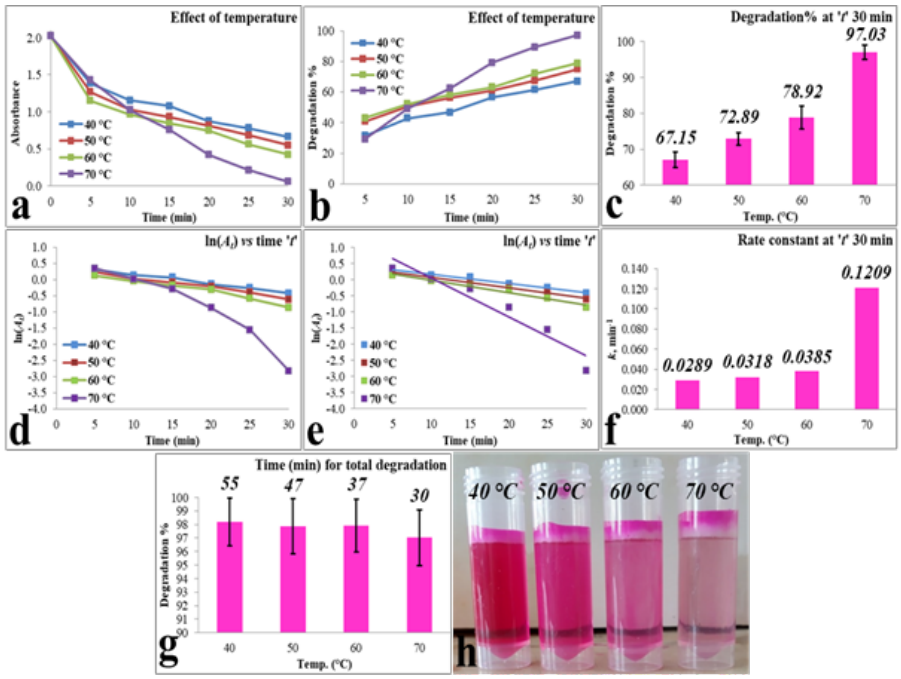

Figure 5: RhB dye degradation at various process temperatures. **(a)** Absorbance values recorded by UV-Vis spec. at 554 nm, **(b)** Degradation% calculated by Eq. 1 (section 2.5.1), **(c)** Degradation% at 30 min, **(d-e)** Ln(A_t) *vs* time '*t*' plot to determine pseudo-first order rate constant, **(f)** Pseudo-first order rate constant values, **(g)** Time taken for total degradation and **(h)** Picture of MO dye degradation at increasing process temperature. *Experimental conditions*: SNPs concentration: 100 µg; SBH concentration: 20 mg; Process temperature: 40 °C, 50 °C, 60 °C and 70 °C; Process pH: 7 and Reaction volume: 5 mL (Stock solutions; SNPs: 2 mg/mL and Dye: 50 mg/100 mL).

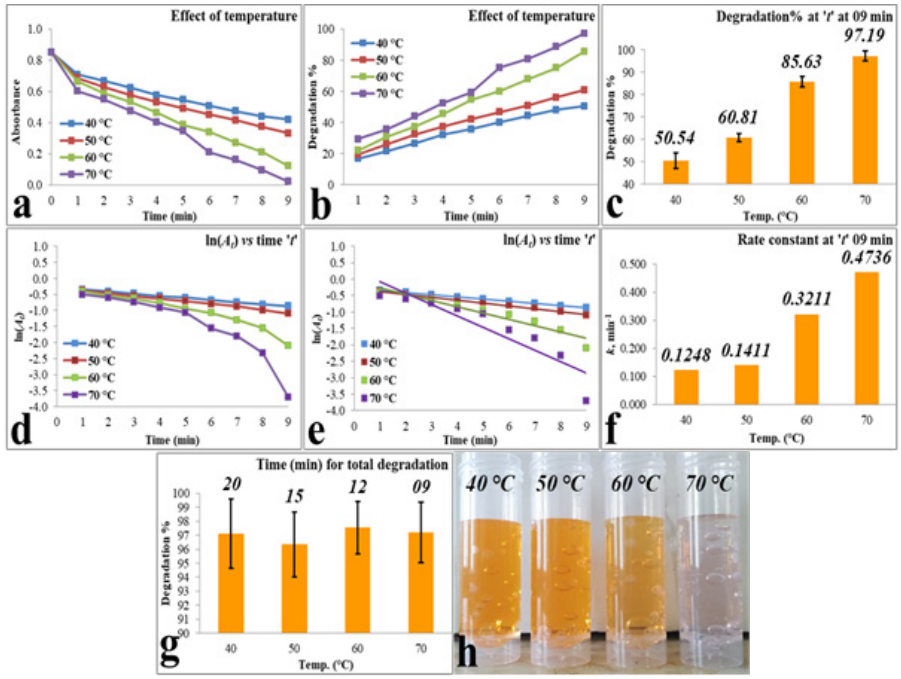

Figure 6: MO dye degradation at various process temperatures. **(a)** Absorbance values recorded by UV-Vis spec. at 464 nm, **(b)** Degradation% calculated by Eq. 1 (section 2.5.1), **(c)** Degradation% at 09 min, **(d-e)** Ln(A_t) *vs* time '*t*' plot to determine pseudo-first order rate constant, **(f)** Pseudo-first order rate constant values, **(g)** Time taken for total degradation and **(h)** Picture of MO dye degradation at increasing process temperature. *Experimental conditions*: SNPs concentration: 100 µg; SBH concentration: 20 mg; Process temperature: 40 °C, 50 °C, 60 °C and 70 °C; Process pH: 7 and Reaction volume: 5 mL (Stock solutions; SNPs: 2 mg/mL and Dye: 50 mg/100 mL).

and SNPs as nano-catalyst.

At pH 6, maximum dye degradation (97.32 ± 2.12%) was observed in less than 7 min with 0.5017 min^{-1} as degradation rate followed by pH 8 with 66.84 ± 2.26% degradation. However, pH 2, pH 4 and pH 10 showed no activity (Figure 8c, 8f and 8h). Total degradation of MO dye was observed under 12 min for pH 6 (97.38 ± 1.75%) with 0.1308 min^{-1} degradation rate (Figure 8c and 8f). Figure 8 presents the details of MO dye degradation at various process pH in the presence of SBH as reducing agent and SNPs as nano-catalyst.

Recyclability

Determining the recyclability of SNPs has great significance such as: (i) making the process cost-effective by reducing the expenses involved in the repeated synthesis of the SNPs and (ii) reduces the amount of SNPs released into the environment thereby reducing the overall toxicity caused by the SNPs on the surrounding ecosystem [36-38]. Recently, several research groups have focussed on the synthesis and preparation of NPs with good catalytic efficiency as well as focussing on their recyclability [39-43] (Table 5). Based on these reasons, the recyclability of SNPs was also investigated in the degradation of RhB and MO dyes in the presence of SBH as reducing agent.

RhB dye

SNPs were determined for their recyclability in the degradation of RhB dye in the presence of SBH as reducing agent based on the physicochemical parameters defined. The experimental conditions were as follows nano-catalyst concentration: 2 mg (defined in section 3.1); reducing agent concentration: 400 mg (defined in section 3.2); process temperature: 70 °C (defined in section 3.3), process pH: 8 (defined in section 3.4) and reaction volume: 100 mL.

SNPs showed good recyclability

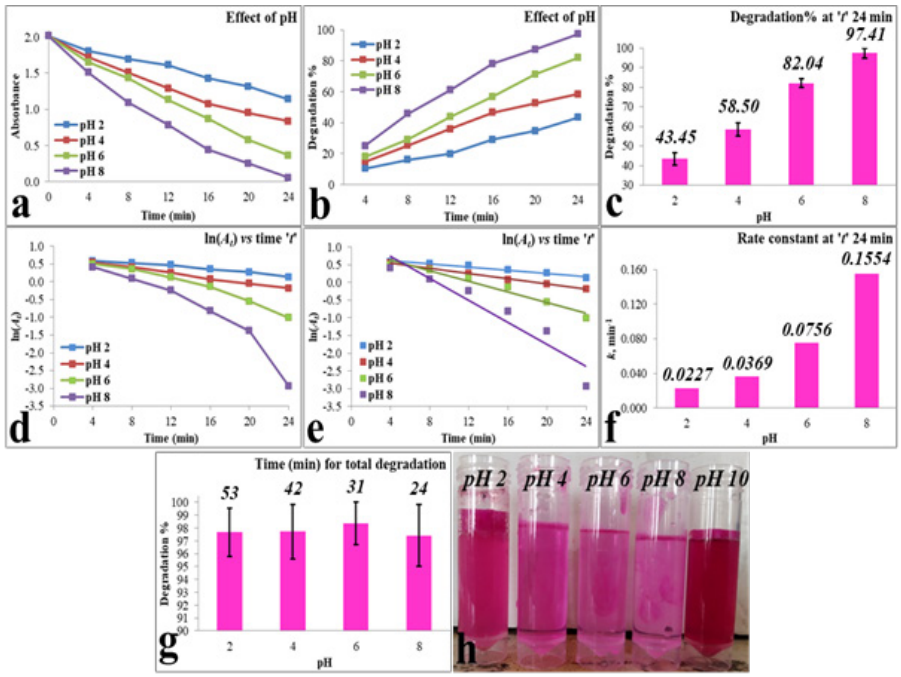

Figure 7: RhB dye degradation at various process pH. **(a)** Absorbance values recorded by UV-Vis spec. at 554 nm, **(b)** Degradation% calculated by Eq. 1 (section 2.5.1), **(c)** Degradation% at 24 min, **(d-e)** Ln(A_t) *vs* time '*t*' plot to determine pseudo-first order rate constant, **(f)** Pseudo-first order rate constant values, **(g)** Time taken for total degradation and **(h)** Picture of MO dye degradation at increasing process pH. *Experimental conditions*: SNPs concentration: 100 µg; SBH concentration: 20 mg; Process temperature: 70 °C; Process pH: 2, 4, 6, 8 and 10 and Reaction volume: 5 mL (Stock solutions; SNPs: 2 mg/mL and Dye: 50 mg/100 mL).

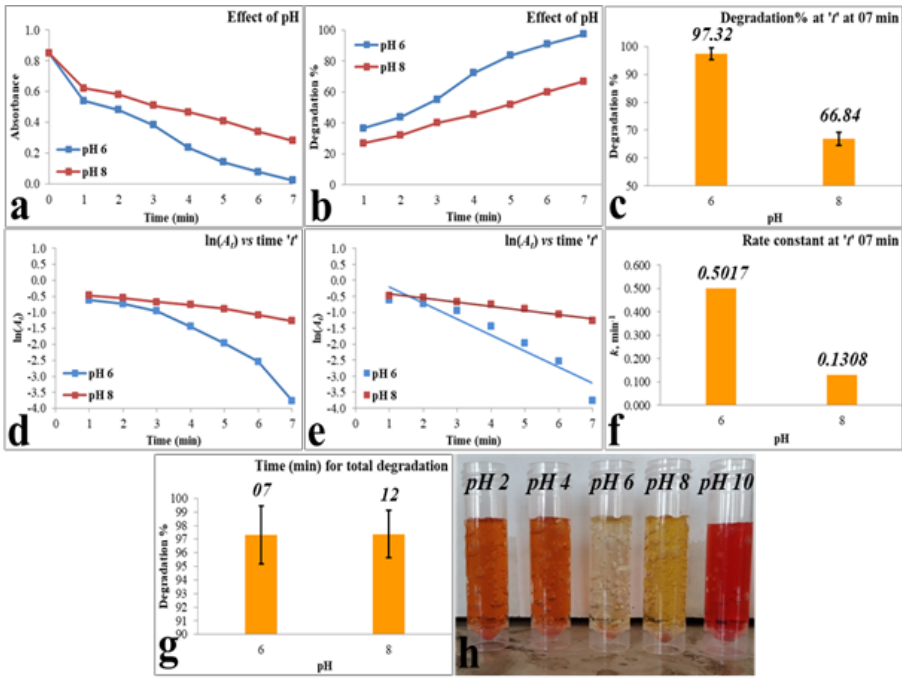

Figure 8: MO dye degradation at various process pH. **(a)** Absorbance values recorded by UV-Vis spec. at 464 nm, **(b)** Degradation% calculated by Eq. 1 (section 2.5.1), **(c)** Degradation% at 07 min, **(d-e)** Ln(A_t) *vs* time '*t*' plot to determine pseudo-first order rate constant, **(f)** Pseudo-first order rate constant values, **(g)** Time taken for total degradation and **(h)** Picture of MO dye degradation at increasing process pH. *Experimental conditions*: SNPs concentration: 100 µg; SBH concentration: 20 mg; Process temperature: 70 °C; Process pH: 2, 4, 6, 8 and 10 and Reaction volume: 5 mL (Stock solutions; SNPs: 2 mg/mL and Dye: 50 mg/100 mL).

till Cycle 2 with 97.14 ± 1.38% for Cycle 0, 97.43 ± 1.87% for Cycle 1 and 96.80 ± 2.42% for Cycle 2 under 24 min with 0.1500 min^{-1}, 0.1526 min^{-1} and 0.1454 min^{-1} as degradation rate constants (pseudo-first order), respectively (Figure 9c and 9f). Whereas, Cycle 3 showed 90.97 ± 2.31% degradation with 0.1005 min^{-1} as degradation rate. After Cycle 3, significant reduction in the activity of SNPs as nano-catalyst was observed. At 24 min, Cycle 4 and Cycle 5 showed only 71.05 ± 2.14% and 52.79 ± 3.19% RhB dye degradation with 0.0556 min^{-1} and 0.0281 min^{-1} as degradation rate constants, respectively (Figure 9c and 9f). Total dye degradation was observed at 28 min, 54 min and 85 min for Cycle 3 (97.03 ± 1.42%), Cycle 4 (97.99 ± 1.16%) and Cycle 5 (97.28 ± 2.36%), respectively (Figure 9g). Figure 9 presents the recyclability details of SNPs as nano-catalysts in the degradation of RhB dye in the presence of SBH as reducing agent. Table 3 presents the experimental conditions under which SNPs recyclability studies were performed in the degradation of RhB dye along with their degradation percentages and rate constants after each cycle.

MO dye

SNPs were determined for their recyclability in the degradation of MO dye in the presence of SBH as reducing agent based on the physicochemical parameters defined. The experimental conditions were as follows nano-catalyst concentration: 2 mg (defined in section 3.1); reducing agent concentration: 400 mg (defined in section 3.2); process temperature: 70 °C (defined in section 3.3), process pH: 6 (defined in section 3.4) and reaction volume: 100 mL.

SNPs showed good recyclability till Cycle 5 with 97.45 ± 1.63% for Cycle 0, 97.41 ± 1.87% for Cycle 1, 98.10 ± 1.14% for Cycle 2, 97.57 ± 2.22% for Cycle 3 and 97.32 ± 1.91% for Cycle 4 under 7 min with 0.5057 min^{-1}, 0.5025 min^{-1}, 0.6141 min^{-1} and 0.5450 min^{-1} as degradation rate constants (pseudo-first

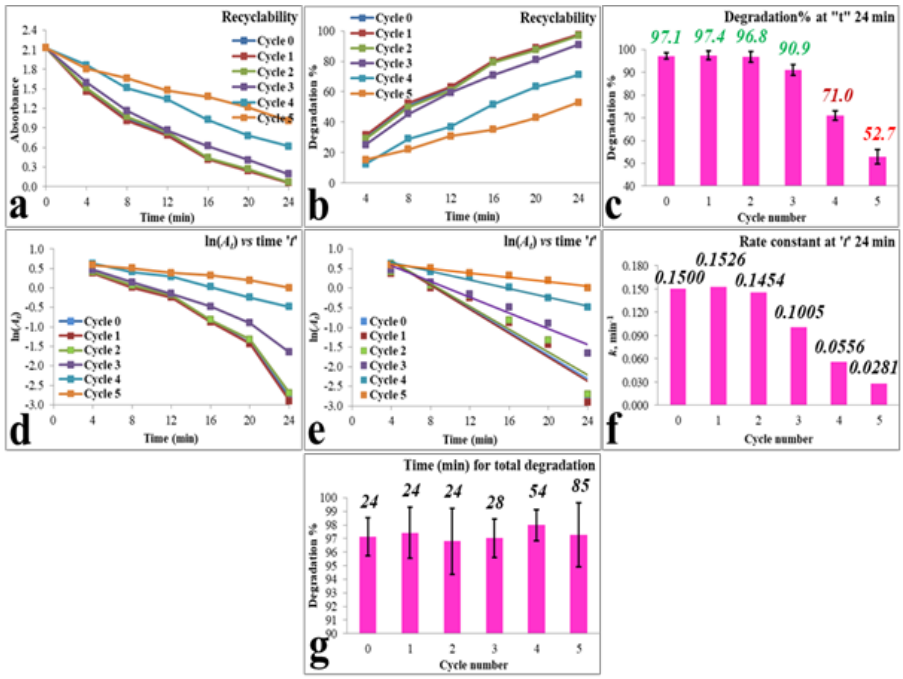

Figure 9: Recyclability of SNPs for the RhB dye degradation in presence of SBH as reducing agent. **(a)** Absorbance values recorded by UV-Vis spec. at 554 nm, **(b)** Degradation% calculated by Eq. 1 (section 2.5.1), **(c)** Degradation% at 24 min, **(d-e)** Ln(A_t) *vs* time '*t*' plot to determine pseudo-first order rate constant, **(f)** Pseudo-first order rate constant values and **(g)** Time taken for total degradation. *Experimental conditions*: SNPs concentration: 2 mg; SBH concentration: 400 mg; Process temperature: 70 °C; Process pH: 8 and Reaction volume: 100 mL (Stock solutions; SNPs: 2 mg/mL and Dye: 50 mg/100 mL).

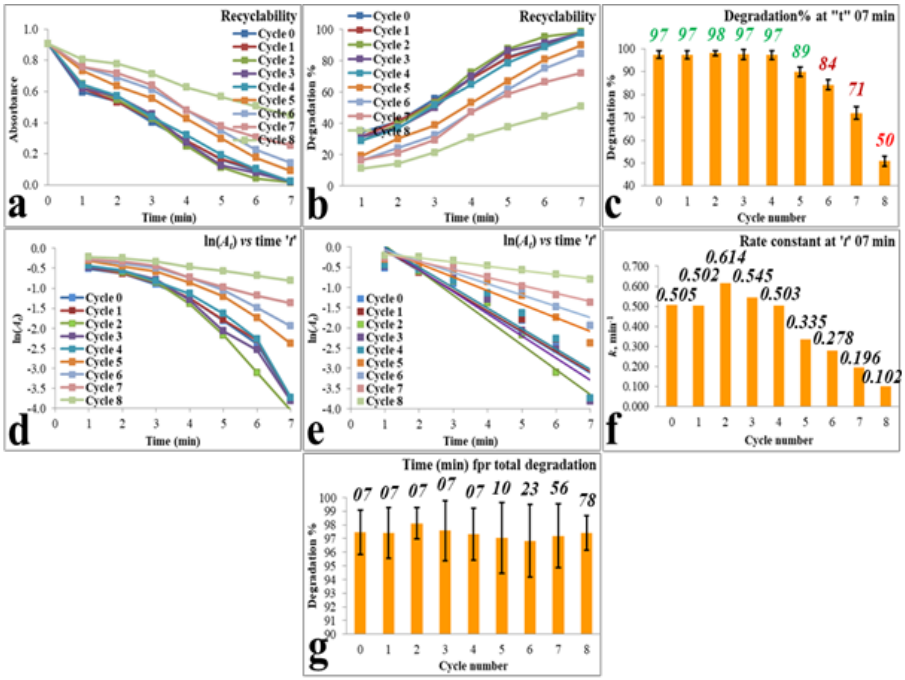

Figure 10: Recyclability of SNPs for the MO dye degradation in presence of SBH as reducing agent. **(a)** Absorbance values recorded by UV-Vis spec. at 464 nm, **(b)** Degradation% calculated by Eq. 1 (section 2.5.1), **(c)** Degradation% at 07 min, **(d-e)** Ln(A_t) *vs* time '*t*' plot to determine pseudo-first order rate constant, **(f)** Pseudo-first order rate constant values and **(g)** Time taken for total degradation. *Experimental conditions*: SNPs concentration: 2 mg; SBH concentration: 400 mg; Process temperature: 70 °C; Process pH: 6 and Reaction volume: 100 mL (Stock solutions; SNPs: 2 mg/mL and Dye: 50 mg/100 mL).

order), respectively (Figure 10c and 10f). Whereas, Cycle 5 and Cycle 6 showed 89.86 ± 2.01% and 84.22 ± 2.19% degradation with 0.3357 min^{-1} and 0.2781 min^{-1} as degradation rates, respectively (Figure 10c and 10f). After Cycle 6, significant reduction in the activity of SNPs as nano-catalyst was observed. At 7 min, Cycle 7 and Cycle 8 showed only 71.95 ± 2.75% and 50.82 ± 2.16% MO dye degradation with 0.1961 min^{-1} and 0.1022 min^{-1} as degradation rate constants, respectively (Figure 10c and 10f). Total dye degradation was observed at 10 min, 23 min, 56 min and 78 min for Cycle 5 (97.05 ± 2.58%), Cycle 6 (96.82 ± 2.65%), Cycle 7 (97.20 ± 2.34%) and Cycle 8 (97.42 ± 1.25%), respectively (Figure 10g). Figure 10 presents the recyclability details of SNPs as nano-catalysts in the degradation of MO dye in the presence of SBH as reducing agent. Table 4 presents the experimental conditions under which SNPs recyclability studies were performed in the degradation of MO dye along with their degradation percentages and rate constants after each cycle.

Future Research and Economical Aspects

Although the present study provides the basic understanding on the overall influence of few physicochemical parameters in the dye degradation process, complexity of the real time environment cannot be replicated or investigated in the laboratory using synthetic wastewater. At present, existing literature also focused on the use of SNPs as photo-catalysts in the degradation of several textile dyes assisted by visible light, irradiation and sunlight or by certain reducing agents. Application of SNPs in real-time scenario is a distant dream, which cannot be fulfilled by the existing experimental approaches due to several limitations: (i) no standard experimental procedure, (ii) unavailability of uniform standards, (iii) presence of diverse or multitude environmental conditions, (iv) presence of other

Table 3: Recyclability of SNPs for RhB dye degradation in presence of SBH as reducing agent.

Dye	Cycle No.	Reaction conditions	Degradation percentage	Rate constant	Correlation coefficient
			(%)	(k), min^{-1}	(R^2)
RhB (50 mg/100 mL)	Cycle 0	SNPs-2mg; SBH-400 mg; Temp-70 °C; pH-8; Time-24 min and Volume-100 mL	97.14 ± 1.38	0.1500	0.9175
	Cycle 1		97.43 ± 1.87	0.1526	0.9097
	Cycle 2		96.80 ± 2.42	0.1454	0.9157
	Cycle 3		90.97 ± 2.31	0.1005	0.9633
	Cycle 4		71.05 ± 2.14	0.0556	0.9880
	Cycle 5		52.79 ± 3.19	0.0281	0.9743

Table 4: Recyclability of SNPs for MO dye degradation in presence of SBH as reducing agent.

Dye	Cycle No.	Reaction conditions	Degradation percentage	Rate constant	Correlation coefficient
			(%)	(k), min^{-1}	(R^2)
MO (50 mg/100 mL)	Cycle 0	SNPs-2 mg; SBH-500 mg; Temp-70 °C; pH-6; Time-7 min and Volume-100 mL	97.45 ± 1.63	0.5057	0.8891
	Cycle 1		97.41 ± 1.87	0.5025	0.8846
	Cycle 2		98.10 ± 1.14	0.6141	0.9334
	Cycle 3		97.57 ± 2.22	0.5450	0.9145
	Cycle 4		97.32 ± 1.91	0.5038	0.8682
	Cycle 5		89.86 ± 2.01	0.3357	0.9222
	Cycle 6		84.22 ± 2.19	0.2781	0.9348
	Cycle 7		71.95 ± 2.75	0.1961	0.9738
	Cycle 8		50.82 ± 2.16	0.1022	0.9841

pollutants or contaminants, which may or may not react or interfere with the SNPs, (v)post-treatment toxicity tests should be performed to assess the structural integrity of SNPs, (vi) should also focus on the structural changes of the dyes during the degradation process and lastly (v) stability and toxicity of the SNPs in actual ecosystem[44-47]. The SNPs might offer an economical and durable approach for the degradation of dyes compared to the conventional approaches. However to determine their real value in the real time environment will not be so cost-effective and can be a dreadful task.

Conclusions

The existing literature has made evident that the dyes used during textile application can be difficult to decolorize because of their chemical structure. Their removal or degradation can be highly specific based on the process employed; therefore, it is a horrendous task to simply choose an approach from the available conventional approaches. Additionally, the conventional physicochemical approaches employed for dye degradation cannot be always efficient, due to several factors such as: concentration of dyes, temperature, pH, presence of other pollutants or contaminants, etc. This has triggered for the development of novel, economical, eco-friendlier, simple yet sophisticated approach. This study aims in the application of SNPs in the degradation of RhB and MO dyes in presence of SBH while investigating the influence of four physicochemical parameters on the degradation process. Recyclability of SNPs was also investigated to make the process more economical, durable and efficient. This study has provide an efficient, durable, recyclable and easily operated degradation process through the application of SNPs as nano-catalysts in the presence of SBH as reducing agent. However, further studies are still required to determine the real time application of the SNPs synthesized in this work.

Acknowledgements

SV and MV thank Department of Chemical Engineering, College of Engineering (A), Andhra University (Visakhapatnam, Andhra Pradesh) for providing the research and laboratory facilities. AV and MS thank the M.H.R.D. for providing

Table 5: Comparison of SNPs recyclability with those reported in literature.

Type		Concentration		Reaction conditions			Remark(s)	Ref.
NPs	Dye	NPs	Dye	pH	Temp.	Vol.		
		mg	mg/L		°C	mL		
AgNPs (SNPs)	RhB and MO	2	500	8 and 6	70	100	52.7 and 50.8% degradation after Cycle 5 and Cycle 8	present work
Ag	RhB and MB	40 µL (2.5 mM)	500	-	-	3	80% degradation after Cycle 4 at 5 min	[48]
ZnO	RhB	-	-	9	room	-	97% degradation after Cycle 5 at 100 min	[49]
Ag@ CeO_2	MO and MB	10	100	-	-	100	85.6 and 88.9% degradation after Cycle 5 at 30 min	[50]
Ag /clinoptilolite	MO, MB, RhB and CR	5	10 ppm	-	room	50	No significant loss of activity after Cycle 6	[51]
Ag-AgCl	RhB and MO	2	500	8 and 6	60	100	72 and 87% degradation after Cycle 4 at 5 and 4 min	[5]
Cu	MO	5	0.03 mM	-	-	3	95% degradation after Cycle 4 at 15 min	[52]

the fellowship. SV thank the R.G.N.F. for providing the fellowship.

Funding

No funding was received for this work.

Conflict of Interest

On behalf of all authors, the corresponding author states that there is no conflict of interest.

Authors' Contribution

Sasikala Vankdoth: Methodology, Experimentation, Data curation, Manuscript-original draft preparation. **Aditya Velidandi:** Conceptualization, Methodology, Experimentation, Data curation, Manuscript-original draft preparation, reviewing and editing. **Mounika Sarvepalli:** Experimentation, Manuscript-reviewing and editing. **Dr. Meena Vangalapati**: Supervision, Manuscript-reviewing and editing. All the authors read and approved the manuscript for submission.

References

1. Hassan SS, Carlson K, Mohanty SK, Canlier SA. 2018. Ultra-rapid catalytic degradation of 4-nitrophenol with ionic liquid recoverable and reusable ibuprofen derived silver nanoparticles. *Environ Pollut* 237: 731-739.https://doi.org/10.1016/j.envpol.2017.10.118
2. Santhosh AS, Sandeep S, Swamy NK. 2019. Green synthesis of nano silver from *euphorbia geniculata* leaf extract: Investigations on catalytic degradation of methyl orange dye and optical sensing of Hg^{2+}.*Surf Interfaces* 14: 50-54.https://doi.org/10.1016/j.surfin.2018.11.004
3. Chand K, Jiao C, Lakhan MN, Shah AH, Kumar V, et al. 2021. Green synthesis, characterization and photocatalytic activity of silver nanoparticles synthesized with *Nigella Sativa* seed extract. *Chem Phys Lett* 763: 138218.https://doi.org/10.1016/j.cplett.2020.138218
4. Velidandi A, Dahariya S, Pabbathi NPP, Kalivarathan D, Baadhe RR. 2020. A review on synthesis, applications, toxicity, risk assessment and limitations of plant extracts synthesized silver nanoparticles. *Nano World J* 6(3): 35-60.https://doi.org/10.17756/nwj.2020-079
5. Velidandi A, Pabbathi NPP, Baadhe RR.2021. Study of parameters affecting the degradation of rhodamine-B and methyl orange dyes by *Annona muricata* leaf extract synthesized nanoparticles as well as their recyclability. *J Mol Struct* 1236: 130287.https://doi.org/10.1016/j.molstruc.2021.130287
6. Textile Dyes Market 2021-2025 with top countries data: industry insights by players, regional segmentation, growth, applications, major drivers, value and foreseen.
7. Khatoon UT, Rao GVSN, Mantravadi KM, Oztekin Y. 2018. Strategies to synthesize various nanostructures of silver and their applications - a review. *RSC Adv* 8: 19739-19753.https://doi.org/10.1039/c8ra00440d
8. Zafar N, Shamaila S, Nazir J, Sharif R, Shahid Rafique M, et al.2016. Antibacterial action of chemically synthesized and laser generated silver nanoparticles against human pathogenic bacteria. *J Mater SciTechnol* 32(8): 721-728.https://doi.org/10.1016/j.jmst.2016.05.009
9. Dada AO, Inyinbor AA, Idu EI, Bello OM, Oluyori AP, et al. 2018. Effect of operational parameters, characterization and antibacterial studies of green synthesis of silver nanoparticles using *Tithonia diversifolia*. *PeerJ* 6: e5865.https://doi.org/10.7717/peerj.5865
10. Marimuthu S, Antonisamy AJ, Malayandi S, Rajendran K, Tsai PC, et al. 2020 Silver nanoparticles in dye effluent treatment: A review on synthesis, treatment methods, mechanisms, photocatalytic degradation, toxic effects and mitigation of toxicity. *J Photochem Photobiol* B Biol 205: 111823.https://doi.org/10.1016/j.jphotobiol.2020.111823
11. Zakaria MA, Menazea AA, Mostafa AM, Al-Ashkar EA. 2020. Ultra-thin silver nanoparticles film prepared via pulsed laser deposition: synthesis, characterization, and its catalytic activity on reduction of 4-nitrophenol. *Surf Interfaces* 19: 100438.https://doi.org/10.1016/j.surfin.2020.100438

12. Velidandi A, Pabbathi NPP, Dahariya S, Baadhe RR. 2021. Green synthesis of novel Ag – Cu and Ag – Zn bimetallic nanoparticles and their in vitro biological, eco-toxicity and catalytic studies. *Nano-Structures & Nano-Objects* 26: 100687.https://doi.org/10.1016/j.nanoso.2021.100687

13. Awad MA, Hendi AA, Ortashi KM, Alzahrani B, Soliman D, et al. 2021. Biogenic synthesis of silver nanoparticles using *Trigonella foenum-graecum* seed extract: characterization, photocatalytic and antibacterial activities. *Sens Actuators A Phys* 323: 112670.https://doi.org/10.1016/j.sna.2021.112670

14. Velidandi A, Pabbathi NPP, Dahariya S, Kagithoju S, Baadhe RR. 2021. Bio-fabrication of silver-silver chloride nanoparticles using *Annona muricata* leaf extract: characterization, biological, dye degradation and eco-toxicity studies. *Int J Environ Sci Technol* 1-18.https://doi.org/10.1007/s13762-021-03461-5

15. Velidandi A, Sarvepalli M, Pabbathi NPP, Baadhe RR. 2021. Biogenic synthesis of novel platinum-palladium bimetallic nanoparticles from aqueous *Annona muricata* leaf extract for catalytic activity. *3 Biotech* 11: 1-14.https://doi.org/10.1007/s13205-021-02935-0

16. Okpara EC, Ogunjinmi OE, Oyewo OA, Fayemi OE, Onwudiwe DC.2021. Green synthesis of copper oxide nanoparticles using extracts of *Solanum macrocarpon* fruit and their redox responses on SPAu electrode. *Heliyon* 7(12): e08571.https://doi.org/10.1016/j.heliyon.2021.e08571

17. Chakraborty B, Kumar RS, Almansour AI, Kotresha D, Rudrappa M, et al. Evaluation of antioxidant, antimicrobial and antiproliferative activity of silver nanoparticles derived from *Galphimia glauca* leaf extract. *J King Saud Univ Sci* 33: 101660.https://doi.org/10.1016/j.jksus.2021.101660

18. Velidandi A, Pabbathi NPP, Dahariya S, Baadhe RR. 2020. Catalytic and eco-toxicity investigations of bio-fabricated monometallic nanoparticles along with their anti-bacterial, anti-inflammatory, anti-diabetic, anti-oxidative and anti-cancer potentials. Colloid Interface Sci Commun 38: 100302.https://doi.org/10.1016/j.colcom.2020.100302

19. Mondal A, Adhikary B, Mukherjee D. 2015. Room-temperature synthesis of air stable cobalt nanoparticles and their use as catalyst for methyl orange dye degradation. *Colloids Surf A Physicochem Eng Asp* 482: 248-257.https://doi.org/10.1016/j.colsurfa.2015.05.011

20. Nasrollahzadeh M, Atarod M, Jaleh B, Gandomirouzbahani M. 2016. In situ green synthesis of Ag nanoparticles on graphene oxide/TiO_2 nanocomposite and their catalytic activity for the reduction of 4-nitrophenol, congo red and methylene blue. *Ceram Int* 42(7): 8587–8596. https://doi.org/10.1016/j.ceramint.2016.02.088

21. Chand K, Cao D, Fouad DE, Shah AH, Lakhan MN, et al. 2020. Photocatalytic and antimicrobial activity of biosynthesized silver and titanium dioxide nanoparticles: a comparative study. *J Mol Liq* 316: 113821. https://doi.org/10.1016/j.molliq.2020.113821

22. Lakhan MN, Chen R, Shar AH, Chand K, Shah AH, et al. 2020. Eco-friendly green synthesis of clove buds extract functionalized silver nanoparticles and evaluation of antibacterial and antidiatom activity. *J Microbiol Methods* 173: 105934.https://doi.org/10.1016/j.mimet.2020.105934

23. Shyamala R, Gomathi Devi LN. 2020. Surface plasmon resonance effect of Ag metallized SnO_2 particles: Exploration of metal induced gap states and characteristic properties of Ohmic junction. *Surf Interface Anal* 52(6): 374–385.https://doi.org/10.1002/sia.6745

24. Vankdoth S, Velidandi A, Sarvepalli M, Vangalapati M. 2022. Role of plant (tulasi, neem and turmeric) extracts in defining the morphological, toxicity and catalytic properties of silver nanoparticles. *Inorg Chem Commun* 140: 109476.https://doi.org/10.1016/j.inoche.2022.109476

25. Kosa SA, Zaheer Z. 2021. Biogenic fabrication of silver nanoparticles, oxidative dissolution and antimicrobial activities. *J Saudi Chem Soc*26(1): 101414.https://doi.org/10.1016/j.jscs.2021.101414

26. Nagasundari SM, Murugan K, Jeyakumar P, Muthu K. 2021. Plant (*Pedalium murex* L.) mucilage green synthesized and capped silver nanoparticles: in vitro biological and solar-driven photocatalytic dye degradation activity. *Phosphorus Sulfur Silicon Relat Elem* 197(3): 254-262.https://doi.org/10.1080/10426507.2021.2012675

27. Khan ZUH, Shah NS, Iqbal J, Khan AU, Imran M, et al. 2020. Biomedical and photocatalytic applications of biosynthesized silver nanoparticles: ecotoxicology study of brilliant green dye and its mechanistic degradation pathways. *J Mol Liq* 319: 114114.https://doi.org/10.1016/j.molliq.2020.114114

28. David L, Moldovan,B. 2020. Green synthesis of biogenic silver nanoparticles for efficient catalytic removal of harmful organic dyes. *Nanomaterials (Basel)* 10(2): 202.https://doi.org/10.3390/nano10020202

29. Naseem K, Ur Rehman MZ, Ahmad A, Algarni TS, Dubal D. 2020. Plant extract induced biogenic preparation of silver nanoparticles and their potential as catalyst for degradation of toxic dyes. Coatings. 10(12): 1-15.https://doi.org/10.3390/coatings10121235

30. Naseem K, Farooqi ZH, Begum R, Irfan A. 2018. Removal of congo red dye from aqueous medium by its catalytic reduction using sodium borohydride in the presence of various inorganic nano-catalysts: a review. *J Clean Prod* 187: 296-307.https://doi.org/10.1016/j.jclepro.2018.03.209

31. Akbari A, Sabouri Z, Hosseini HA, Hashemzadeh A, Khatami M, et al. 2020. Effect of nickel oxide nanoparticles as a photocatalyst in dyes degradation and evaluation of effective parameters in their removal from aqueous environments. *Inorg Chem Commun* 115: 107867.https://doi.org/10.1016/j.inoche.2020.107867

32. Sabouri Z, Akbari A, Hosseini HA, Hashemzadeh A, Darroudi M. 2019. Bio-based synthesized NiO nanoparticles and evaluation of their cellular toxicity and wastewater treatment effects. *J Mol Struct* 1191: 101-109.https://doi.org/10.1016/j.molstruc.2019.04.075

33. Wang Y, Sun X, Xian T, Liu G, Yang H.2021. Photocatalytic purification of simulated dye wastewater in different pH environments by using $BaTiO_3/Bi_2WO_6$ heterojunction photocatalysts. *Opt Mater* 113: 110853. https://doi.org/10.1016/j.optmat.2021.110853

34. Tang X, Li Z, Liu K, Luo X, He D, et al. 2020. Sulfidation modified Fe_3O_4 nanoparticles as an efficient Fenton-like catalyst for azo dyes degradation at wide pH range. *Powder Technol* 376: 42-51.https://doi.org/10.1016/j.powtec.2020.08.018

35. Nasab NK, Sabouri Z, Ghazal S, Darroudi M. 2020. Green-based synthesis of mixed-phase silver nanoparticles as an effective photocatalyst and investigation of their antibacterial properties. *J Mol Struct* 1203: 127411.https://doi.org/10.1016/j.molstruc.2019.127411

36. Adewunmi AA, Kamal MS, Solling TI. 2021. Application of magnetic nanoparticles in demulsification: A review on synthesis, performance, recyclability, and challenges. *J Pet Sci Eng* 196: 107680.https://doi.org/10.1016/j.petrol.2020.107680

37. Ho TTT, Dang CH, Huynh TKC, Hoang TKD, Nguyen TD.2021. In situ synthesis of gold nanoparticles on novel nanocomposite lactose/alginate: recyclable catalysis and colorimetric detection of Fe(III). *Carbohydr Polym* 251: 116998.https://doi.org/10.1016/j.carbpol.2020.116998

38. Salama RS, El-Sayed ESM, El-Bahy SM, Awad FS.2021. Silver nanoparticles supported on UiO-66 (Zr): As an efficient and recyclable heterogeneous catalyst and efficient adsorbent for removal of indigo carmine. *Colloids Surf A Physicochem Eng Asp* 626: 127089.https://doi.org/10.1016/j.colsurfa.2021.127089

39. Tripathi RM, Chung SJ. 2020. Reclamation of hexavalent chromium using catalytic activity of highly recyclable biogenic Pd(0) nanoparticles. *Sci Rep* 10:640.https://doi.org/10.1038/s41598-020-57548-z

40. Xu P, Wu Z, Dai W, Wang Y, Zheng M, et al. 2021. Synthesis of multiple Ag nanoparticles loaded hollow mesoporous carbon spheres for highly efficient and recyclable catalysis. *Microporous Mesoporous Mater* 314: 110856.https://doi.org/10.1016/j.micromeso.2020.110856

41. Veisi H, Karmakar B, Tamoradi T, Tayebee R, Sajjadifar S, et al. 2021. Bio-inspired synthesis of palladium nanoparticles fabricated magnetic Fe_3O_4 nanocomposite over *Fritillaria imperialis* flower extract as an efficient recyclable catalyst for the reduction of nitroarenes. *Sci Rep* 11:4515.https://doi.org/10.1038/s41598-021-83854-1

42. Yue Y, Wang X, Wu Q, Han J, Jiang J.2020. Highly recyclable and super-tough hydrogel mediated by dual-functional TiO_2 nanoparticles toward efficient photodegradation of organic water pollutants. *J Colloid Interface Sci* 564: 99-112.https://doi.org/10.1016/j.jcis.2019.12.069

43. Doan VD, Phung MT, Nguyen TLH, Mai TC, Nguyen TD.2020. Noble metallic nanoparticles from waste *Nypa fruticans* fruit husk: Biosynthesis, characterization, antibacterial activity and recyclable catalysis. *Arab J Chem* 13: 7490-7503.https://doi.org/10.1016/j.arabjc.2020.08.024

44. Fawzi Suleiman Khasawneh O, Palaniandy P. 2021. Removal of organic pollutants from water by Fe_2O_3/TiO_2 based photocatalytic degradation: a review. *Environ Technol Innov* 21: 101230. https://doi.org/10.1016/j.eti.2020.101230

45. Hitam CNC, Jalil AA. A review on exploration of Fe_2O_3 photocatalyst towards degradation of dyes and organic contaminants. *J Environ Manage* 258: 110050.https://doi.org/10.1016/j.jenvman.2019.11005

46. Nemiwal M, Zhang TC, Kumar D.2021. Recent progress in g-C_3N_4, TiO_2 and ZnO based photocatalysts for dye degradation: Strategies to improve photocatalytic activity. *Sci Total Environ* 767: 144896.https://doi.org/10.1016/j.scitotenv.2020.144896

47. Mmelesi OK, Masunga N, Kuvarega A, Nkambule TT, Mamba BB, et al. 2021. Cobalt ferrite nanoparticles and nanocomposites: Photocatalytic, antimicrobial activity and toxicity in water treatment. *Mater Sci Semicond Process* 123: 105523.https://doi.org/10.1016/j.mssp.2020.105523

48. Pandey S, Do JY, Kim J, Kang M. 2020. Fast and highly efficient catalytic degradation of dyes using κ-carrageenan stabilized silver nanoparticles nanocatalyst. *Carbohydr Polym* 230: 115597.https://doi.org/10.1016/j.carbpol.2019.115597

49. Rafique M, Tahir R, Gillani SSA, Tahir MB, Shakil M, et al.2020. Plant-mediated green synthesis of zinc oxide nanoparticles from *Syzygium Cumini* for seed germination and wastewater purification. *Int J Environ Anal Chem*102(1):1-16.https://doi.org/10.1080/03067319.2020.1715379

50. Ayodhya D, Veerabhadram G. 2020. Green synthesis of garlic extract stabilized Ag@CeO_2 composites for photocatalytic and sonocatalytic degradation of mixed dyes and antimicrobial studies. *J Mol Struct* 1205: 127611.https://doi.org/10.1016/j.molstruc.2019.127611

51. Khodadadi B, Bordbar M, Yeganeh-Faa A, Nasrollahzadeh M. 2017. Green synthesis of Ag nanoparticles/clinoptilolite using *Vaccinium macrocarpon* fruit extract and its excellent catalytic activity for reduction of organic dyes. *J Alloys Compd* 719: 82-88.https://doi.org/10.1016/j.jallcom.2017.05.135

52. Ismail M, Gul S, Khan MI, Khan MA, Asiri AM, et al. 2019. Green synthesis of zerovalent copper nanoparticles for efficient reduction of toxic azo dyes congo red and methyl orange. *Green Process Synth* 8(1): 135-143. https://doi.org/10.1515/gps-2018-0038